Roohalamin Zeinali Davarani[1,*], Reza Ghazi[2]

J. Electrical Systems 9-4 (2013): 410-421

Regular paper

Optimal simultaneous coordination of PSS and TCSC using multi objective genetic algorithm

JES
Journal of Electrical Systems

Power system stability enhancement via optimal simultaneous coordinated design of a power system stabilizer (PSS) and a thyristor-controlled series capacitor (TCSC) for electric power systems oscillations damping is investigated in this paper. A SMIB system equipped with PSS and TCSC controllers is considered in this study. Although these controllers are used for stabilization of power system oscillations but the system must preserve its stability when subjected to sever disturbances. Therefore, the overall stability of the system should be considered. To do so, in the present paper the problem of controllers design is formulated as a multi objective optimization problem. Then the multi objective genetic algorithm (MOGA) is explored to solve this optimization problem. Pareto method type of selection is used in the present MOGA approach.

Keywords: Power system stabilizer, Thyristor-controlled series capacitor, Multi objective genetic algorithm.

1. Introduction

Power systems are more loaded than before due to the restriction on transmission and generation expansion. As a result, they are operated near their stability limits. The poorly damped power system oscillations may result in loss of stability. Power system stabilizers (PSS) have been used for damping low frequency oscillations and so enhancing the power system stability. In addition to PSSs, which are the power system primary oscillation damping controls, the Flexible AC Transmission Systems (FACTS) are applied to network to enhance the stability performance of power system and improve damping of oscillations. The power system stability and its performance can be improved by simultaneous use of PSS and FACTS devices. TCSC is one of the most promising device in FACTS family serve as a supplementary damping controller.

Coordination between PSS and FACTS device is important, because uncoordinated control of these controllers may bring about instability performance of power systems. Although many researches have been done on this subject but in all of them only dynamic stability is considered as an objective function. Although the dynamic stability can be improved by PSS, but in some situations where the system is subjected to severe disturbances, the transient stability may be adversely affected. Therefore, the overall system stability to be considered as an objective function so that for all conditions, the dynamic stability is provided and the transient stability is not jeopardized. Several robust and optimization approaches have been used in the literature. To do so, in this paper the synchronizing and damping torques are considered as objective functions. The design problem of coordination of PSS and TCSC controllers is transferred into a multi objective optimization problem. Then the Multi Objective Genetic Algorithm (MOGA) is employed

[*] R. Zeinali Davarani, Graduate University of Advanced Technology, Haftbagh highway, Kerman, Iran, E-mail: r.zeinali@kgut.ac.ir
[1] Department of Electrical Engineering, Graduate University of Advanced Technology, Iran
[2] Department of Electrical Engineering, Ferdowsi University of Mashhad, Iran

to search for the optimal settings of PSS and TCSC controller's parameters. Pareto method type selection is used in the present MOGA to solve the multi objective optimization problem. In this method, instead of selecting and reproducing only the best solution in general, a set of solutions is produced based on the values of all the different objectives that considered in optimization problem. This set is called Pareto front and any solution of this front demonstrates special case so that none of the objective functions can further improved without deteriorating the other objective at the same time.

The rest of this paper is organized as follows. In Section 2, the equations describing the dynamic behaviour of the SMIB system equipped with TCSC are briefly introduced. Section 3 is devoted to the explanation of the proposed approach. In Section 4, the structure of the multi objective genetic algorithm is described. Section 5 shows the tests and the results obtained from the designed controllers. Finally, conclusions are given in Section 6.

2. Notation

The notation used throughout the paper is stated below.

Indexes:

K_d	damping torque coefficient
K_s	synchronizing torque coefficient
V_{ref}	reference voltage for the excitation system
V_s	stabilizing signal from the PSS
V_T	generator terminal voltage
X_{TCSC}	reactance of TCSC
α	firing angle of thyristors
σ	conduction angle of thyristors

Constants:

D	damping constant of generator
H	inertia constant of generator
K_A	gain of the excitation system
T_A	time constant of the excitation system
T'_{do}	transient time constant of generator
X_C	reactance of the capacitor in TCSC
X_d	d-axis reactance of generator
X'_d	transient time constant of generator
X_q	q-axis reactance of generator
X_L	reactance of the transmission line
X_P	reactance of the reactor in TCSC
X_T	reactance of the transformer

3. Power system model

3.1. Single machine infinite bus

In this study a SMIB power system equipped with PSS and a TCSC which is installed in the transmission line is considered as shown in Fig.1. The synchronous machine is modeled by the two-axis model [11]. The transmission line is modeled by the reactance X_L and the reactance X_T represents the reactance of transformer, V_T and V_B are the generator bus and infinite bus voltage respectively.

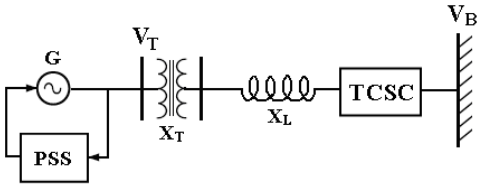

Fig. 1. Single machine infinite bus power system with PSS and TCSC

In this study the IEEE Type-ST1A excitation system is considered and its block diagram is shown in Fig. 2. In the figure V_T is the generator terminal, V_{ref} is the reference voltage for the excitation system and V_s is the stabilizing signal from the PSS. Also K_A and T_A are the gain and time constant of the excitation system respectively.

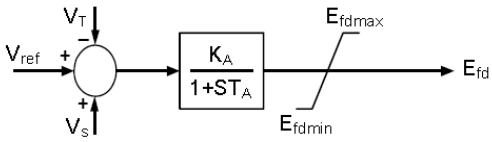

Fig. 2. IEEE Type-ST1A excitation system with PSS signal

3.2. Power system stabilizer

The widely used lead-lag controller shown in Fig. 3 is chosen in this study. The machine speed is considered as stabilizer signal input.

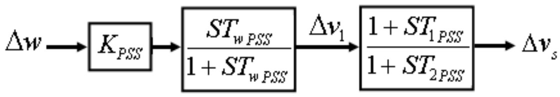

Fig. 3. Block diagram of PSS

3.3. Thyristor-controlled series capacitor

The equivalent circuit of a typical TCSC is shown in Fig. 4. It consists of a fixed series capacitor (C) in parallel with a thyristor controlled reactor.

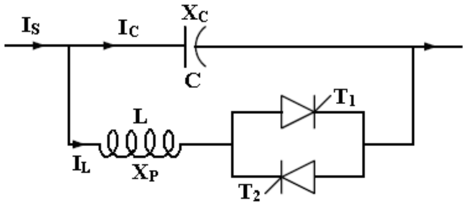

Fig. 4. Basic structure of a TCSC

In the figure X_C and X_P represent the reactance of capacitor and reactor respectively. The reactor (L) is controlled by a bi-directional thyristors (T_1 and T_2). The firing angle of thyristors α is controlled with respect to some system parameter variations such as voltage or current of transmission lines. The angle α can vary from 90 to 180 degree to adjust the

TCSC reactance in accordance with a system control algorithm. The conduction angle σ is defined as $\sigma = 2(\pi - \alpha)$. For $\sigma = 0$, TCSC modeled by X_C (X_{TCSC}=X_C), and for $\sigma = \pi$ the TCSC is modeled by X_C parallel with X_P (X_{TCSC}=X_C||X_P=X_C*X_P/(X_C-X_P)). For other value of α the reactance X_{TCSC} vary from X_C to X_C||X_P. There exists a steady-state relationship between the firing angle α and the reactance X_{TCSC}. This relationship can be described by the following equation [12]:

$$X_{TCSC}(\sigma) = X_C - \left(\frac{X_C^2}{X_C - X_P}\right)\left(\frac{\sigma + \sin(\sigma)}{\pi}\right) + \left(\frac{4X_C^2}{X_C - X_P}\right)\left(\frac{\cos^2(\sigma/2)}{k^2 - 1}\right)\left(\frac{k\tan(k\sigma/2) - \tan(\sigma/2)}{\pi}\right) \tag{1}$$

where

$$k = \sqrt{\frac{X_C}{X_P}} \qquad \sigma = 2(\pi - \alpha) \tag{2}$$

The commonly used lead–lag structure of a TCSC controller is shown in Fig. 5

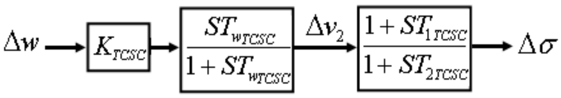

Fig.5. Block diagram of TCSC controller

3.4. Linearized model

In the design of damping controllers, a linearized model of a power system is employed [6, 13]. The non linear dynamic equation can be linearized around a given operating point, so the following are given:

$$\begin{aligned}
\Delta\dot{w} &= \frac{1}{M}\left(-K_1\Delta\delta - D\Delta w - K_2\Delta E_q^{'} - K_p\Delta\sigma + \Delta P_m\right) \\
\Delta\dot{\delta} &= w_0\Delta w \\
\Delta\dot{E}_q^{'} &= \frac{1}{T_{do}^{'}}\left(-K_4\Delta\delta + \Delta E_{fd} - K_3\Delta E_q^{'} - K_q\Delta\sigma\right) \\
\Delta\dot{E}_{fd} &= \frac{K_A}{T_A}\left(V_{ref} - K_5\Delta\delta - \Delta E_{fd}/K_A - K_6\Delta E_q^{'} - K_v\Delta\sigma\right) \\
\Delta\dot{v}_1 &= \frac{K_{PSS}}{M}\left(-D\Delta w - K_1\Delta\delta - K_2\Delta E_q^{'} - K_p\Delta\sigma + \Delta P_m\right) - \Delta v_1/T_{wPSS} \\
\Delta\dot{v}_s &= \frac{1}{T_{2PSS}}\left[\frac{T_{1PSS}K_{PSS}}{M}\left(-D\Delta w - K_1\Delta\delta - K_2\Delta E_q^{'} - K_p\Delta\sigma + \Delta P_m\right) + \left(1 - \frac{T_{1PSS}}{T_{wPSS}}\right)\Delta v_1 - \Delta v_s\right] \\
\Delta\dot{v}_2 &= \frac{K_{TCSC}}{M}\left(-K_1\Delta\delta - D\Delta w - K_2\Delta E_q^{'} - K_p\Delta\sigma + \Delta P_m\right) - \Delta v_2/T_{wTCSC}
\end{aligned} \tag{3}$$

$$\dot{\Delta\sigma} = \frac{1}{T_{2TCSC}}\left[\frac{T_{1TCSC}K_{TCSC}}{M}\left(-D\Delta w - K_1\Delta\delta - K_2\Delta E'_q + \Delta P_m\right) + \left(1 - \frac{T_{1TCSC}}{T_{wTCSC}}\right)\Delta v_2 - \left(1 + \frac{T_{1TCSC}K_{TCSC}K_p}{M}\right)\Delta v_\sigma\right]$$

where

$$\begin{aligned} &K_1 = \partial P_e/\partial\delta,\ K_2 = \partial P_e\big/\partial E'_q,\ K_3 = \partial E_q\big/\partial E'_q,\ K_4 = \partial E_q/\partial\delta,\ K_5 = \partial V_T/\partial\delta,\ K_6 = \partial V_T\big/\partial E'_q, \\ &K_p = \partial P_e/\partial\sigma,\ K_q = \partial E_q/\partial\sigma,\ K_v = \partial V_T/\partial\sigma \end{aligned} \tag{4}$$

and

$$\begin{aligned} P_e &= \frac{E'_q V_B}{X_{d\Sigma'}}\sin\delta - \frac{V_B^2\left(X_q - X'_d\right)}{2X_{d\Sigma'}X_{q\Sigma'}}\sin 2\delta \\ E_q &= \frac{X_{d\Sigma}E'_q}{X_{d\Sigma'}} - \frac{V_B\left(X_d - X'_d\right)}{X_{d\Sigma'}}\cos\delta \\ V_T &= \sqrt{V_{Td}^2 + V_{Tq}^2} \\ V_{Td} &= \frac{X_q V_B}{X_{q\Sigma'}}\sin\delta \\ V_{Tq} &= \frac{X_{Eff}E'_q}{X_{d\Sigma'}} + \frac{X'_d V_B}{X_{d\Sigma'}}\cos\delta \end{aligned} \tag{5}$$

and

$$\begin{aligned} X_{d\Sigma'} &= X'_d + X_{Eff} \\ X_{q\Sigma'} &= X_q + X_{Eff} \\ X_{d\Sigma} &= X_d + X_{Eff} \\ X_{Eff} &= X_T + X_L - X_{TCSC} \end{aligned} \tag{6}$$

The Phillips-Heffron model of the SMIB system with PSS and TCSC obtained from the linearized equations (1)-(6) is shown in Fig. 6. In the figure G_{PSS} and G_{TCSC} represent the transfer function of PSS and TCSC controllers respectively and expressed as follows:

$$\begin{aligned} G_{PSS} &= K_{PSS}\left(\frac{ST_{wPSS}}{1 + ST_{wPSS}}\right)\left(\frac{1 + ST_{1PSS}}{1 + ST_{2PSS}}\right) \\ G_{TCSC} &= K_{TCSC}\left(\frac{ST_{wTCSC}}{1 + ST_{wTCSC}}\right)\left(\frac{1 + ST_{1TCSC}}{1 + ST_{2TCSC}}\right) \end{aligned} \tag{7}$$

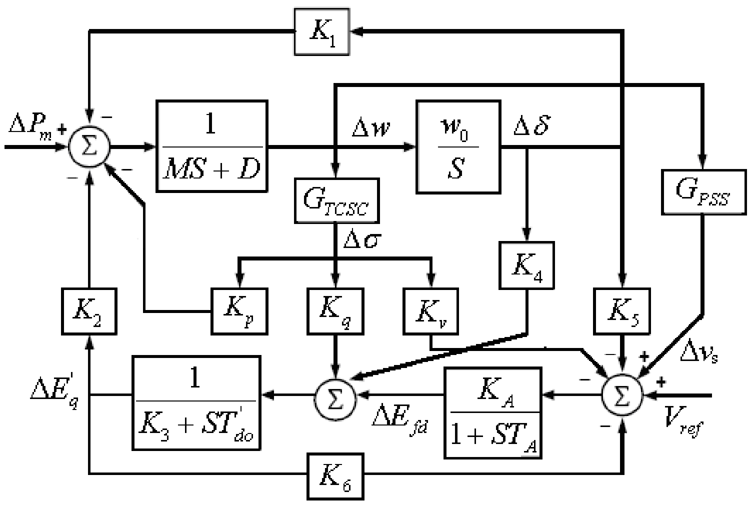

Fig. 6. The Phillips-Heffron block diagram model of the SMIB system with PSS and TCSC

4. The proposed approach

For achieving the simultaneous operation of PSS and TCSC controllers, the damping and synchronizing torques are considered as objective functions. From fig.6 we can write:

$$\Delta P_e = \left[K_1 - \frac{K_2}{K_3 + ST'_{do} + K_6 Ge_x}(G_{ex}K_5 + K_4)\right]\Delta\delta + \left[\frac{K_2}{K_3 + ST'_{do} + K_6 Ge_x}\left(G_{ex}G_{PSS} - G_{ex}K_v G_{TCSC} - K_q G_{TCSC}\right) + K_p G_{TCSC}\right]\Delta w \tag{8}$$

In per unit $\Delta T_e = \Delta P_e$ and referring to equation (8) we have:

$$\begin{aligned} \Delta T_e &= \Delta P_e = (a + jb)\Delta\delta + (c + jd)\Delta w \\ \Delta T_e &= \Delta P_e = K_s\Delta\delta + K_d\Delta w \end{aligned} \tag{9}$$

Where K_s and K_d are synchronizing and damping torque coefficients respectively. In equation (9) when b and d are equal to zero, then K_s and K_d can be calculated as follows:

$$\begin{aligned} K_s &= K_1 - \frac{K_2}{K_3 + ST'_{do} + K_6 Ge_x}(G_{ex}K_5 + K_4) \\ K_d &= \frac{K_2}{K_3 + ST'_{do} + K_6 Ge_x}\left(G_{ex}G_{PSS} - G_{ex}K_v G_{TCSC} - K_q G_{TCSC}\right) + K_p G_{TCSC} \end{aligned} \tag{10}$$

When b and d are not equal to zero, K_s and K_d can be calculated with the aid of equation (11).

$$\begin{aligned} &\Delta\dot{\delta} = w_0\Delta w \quad \rightarrow \quad S^*\Delta\delta = w_0\Delta w \\ &S^* = \xi w_n \pm j w_n\sqrt{1-\xi^2} \end{aligned} \tag{11}$$

$$j\Delta\delta = \frac{w_0}{w_n\sqrt{1-\xi^2}}\Delta w - \frac{\xi w_n}{w_n\sqrt{1-\xi^2}}\Delta\delta$$

$$j\Delta w = \frac{b\xi w_n}{w_n\sqrt{1-\xi^2}}\Delta w - \left(\frac{w_n\sqrt{1-\xi^2}}{w_0} + \frac{(\xi w_n)^2}{w_0 w_n\sqrt{1-\xi^2}}\right)\Delta\delta$$

Where S^* is the oscillation frequency of rotor and calculated as follows:

$$(A - SI)\varphi = 0$$

$$\begin{bmatrix} \dot{\Delta w} \\ \dot{\Delta\delta} \\ \dot{\Delta E'_q} \\ \dot{\Delta E_{fd}} \\ \dot{\Delta v_1} \\ \dot{\Delta v_s} \\ \dot{\Delta v_2} \\ \dot{\Delta\sigma} \end{bmatrix} = \underbrace{\begin{bmatrix} a_{11} & . & . & . & . & a_{18} \\ . & & & & & . \\ . & & & & & . \\ . & & & & & . \\ . & & & & & . \\ a_{81} & . & . & . & . & a_{88} \end{bmatrix}}_{A} \begin{bmatrix} \Delta w \\ \Delta\delta \\ \Delta E'_q \\ \Delta E_{fd} \\ \Delta v_1 \\ \Delta v_s \\ \Delta v_2 \\ \Delta\sigma \end{bmatrix} \tag{12}$$

$$\psi = \varphi^{-1}$$

$$P = \underbrace{\begin{bmatrix} \varphi_{11}\psi_{11} & . & . & . & \varphi_{18}\psi_{81} \\ . & & & & . \\ . & & & & . \\ . & & & & . \\ \varphi_{81}\psi_{18} & . & . & . & \varphi_{88}\psi_{88} \end{bmatrix}}_{S_1 \quad . \quad . \quad . \quad S_8} \left\{ \begin{matrix} \Delta w \\ . \\ . \\ . \\ \Delta\sigma \end{matrix} \right.$$

Where P is the participation matrix and in the connected line to Δw the greatest column determines the oscillation frequency S^*.

By substituting $j\Delta\delta$ and $j\Delta w$ from equation (11) into equation (9), K_s and K_d calculated as follows:

$$K_s = a - \frac{b\xi w_n}{w_n\sqrt{1-\xi^2}} - d\left(\frac{w_n\sqrt{1-\xi^2}}{w_0} + \frac{(\xi w_n)^2}{w_0 w_n\sqrt{1-\xi^2}}\right)$$
$$K_d = c + \frac{d\xi w_n}{w_n\sqrt{1-\xi^2}} + \frac{b w_0}{w_n\sqrt{1-\xi^2}} \tag{13}$$

The problem is formulated so as to maximize the following objective function:

$$J = (f_1, f_2) \tag{14}$$

where

$$f_1 = K_s$$
$$f_2 = K_d \tag{15}$$

The problem constraints are the PSS and TCSC controller's parameters limits. Therefore, the design problem can be formulated as the following optimization problem:

$$\begin{aligned}
&\text{Maximize } J \\
&\quad \text{subject to} \\
&K_{PSS}^{min} < K_{PSS} < K_{PSS}^{max} \\
&T_{1PSS}^{min} < T_{1PSS} < T_{1PSS}^{max} \\
&T_{2PSS}^{min} < T_{2PSS} < T_{2PSS}^{max} \\
&K_{TCSC}^{min} < K_{TCSC} < K_{TCSC}^{max} \\
&T_{1TCSC}^{min} < T_{1TCSC} < T_{1TCSC}^{max} \\
&T_{2TCSC}^{min} < T_{2TCSC} < T_{2TCSC}^{max}
\end{aligned} \tag{16}$$

To solve this optimization problem multi objective genetic algorithm is employed. Using this algorithm an optimal set of PSS and TCSC controller's parameters is obtained.

5. Multi objective genetic algorithm

In recent years, GA has been widely used for combinational optimization, numerical optimization and many other engineering problems [15]. GA involves three operations as Selection, Crossover, and Mutation. The goal of selection is to determine the best chromosomes to retain or worse chromosomes to delete for each generation based on fitness function. The flowchart of GA is shown in Fig. 7.

In many real-world engineering optimization problems there are several conflicting objectives. In many cases, multiple objective problems are considered into one single objective function by selecting weights, but in this case in addition we can not analyze objective function separately. In some problems aggregating multi objective function into one objective function is very difficult. Also, design engineers are often interested in identifying a Pareto optimal set of alternatives when exploring a design space. Pareto optimality is defined as a set where every element is a problem solution for which no other solutions can be better in all design attributes. For example for the two dimensional case, the Pareto front is a curve that clearly illustrates the trade-off between the objectives. When GA is applied to multi objective optimization to obtain Pareto optimal set it called MOGA.

The most important problem must be considered when a GA is applied to a multi objective optimization problem is that how to calculate fitness function for each solution and how to select best solution in order to guide the search to Pareto optimal set.

To solve this problem some techniques is presented such as VEGA[1], HLGA[2], FFGA,[3] and SPEA[4]. In this paper FFGA method is used to obtain Pareto front, in this technique Pareto optimal set is obtained by ranking each solution [16].

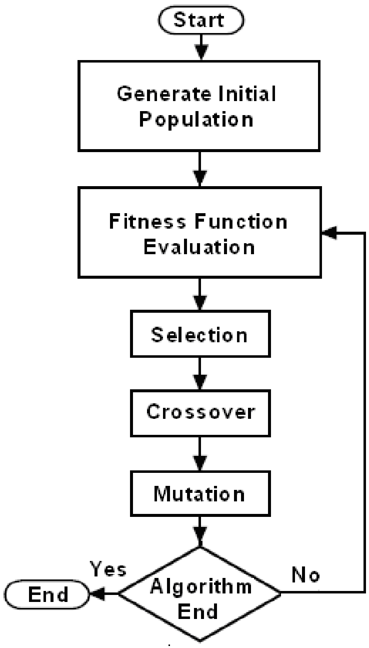

Fig. 7. Flowchart of the GA

6. Test and results

To evaluate the proposed approach first we should specify the parameters which are used in genetic algorithm and the constraints associated with the objective function. Table 1 shows the GA parameters and Table 2 show the limits corresponding to PSS and TCSC controllers.

Table 1. GA parameters

Parameter	Value
Maximum generations	120
Population size	40
Crossover rate	0.7
Mutation rate	0.1

Table 2. Limits on PSS and TCSC controllers

Parameters	K_{PSS}	T_{1PSS}	T_{2PSS}	K_{TCSC}	T_{1TCSC}	T_{2TCSC}
Minimum range	0	0.1	0.01	0	0.1	0.01
Maximum range	15	0.5	0.05	15	0.5	0.05

The optimal set of solution of equation (14) obtained by MOGA based Pareto front shown in Fig. 8.

[1] Vector Evaluated Genetic Algorithm
[2] Hajla and lin's Weighting-based Genetic Algorithm
[3] Fonseca and Fleming's Multi objective Genetic Algorithm
[4] Strength Pareto Evolutionary Algorithm

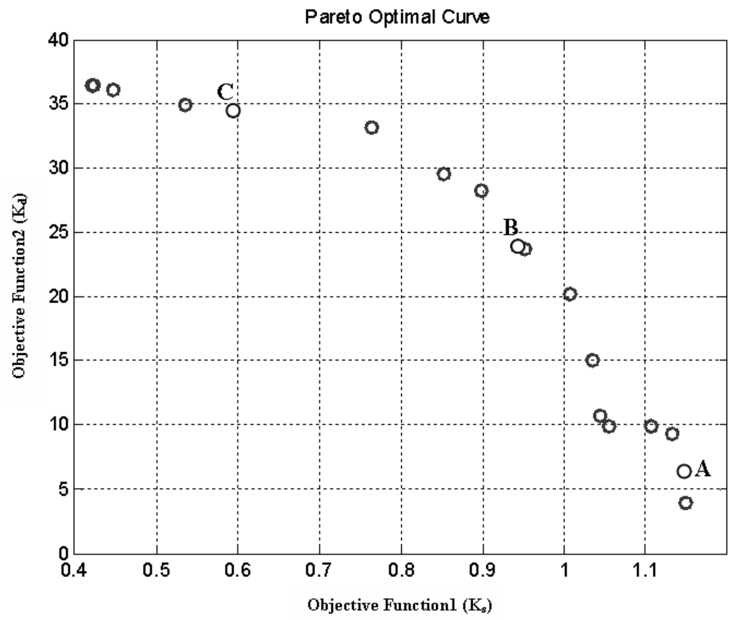

Fig. 8. A set of solution for optimization problem

The value of PSS and TCSC controller's parameters for three situations A, B and C are shown in Table 3.

Table 3. The value of PSS and TCSC controller's parameters for three situations A, B and C

situation	K_{PSS}	T_{1PSS}	T_{2PSS}	K_{TCSC}	T_{1TCSC}	T_{2TCSC}
A	2.1	0.12	0.025	0.3	0.17	0.048
B	8.4	0.15	0.044	0.45	0.16	0.033
C	12.7	0.13	0.048	6.9	0.12	0.049

The results illustrate that as expected when PSS and TCSC controllers gains are adjusted at small value, the damping torque is negligible and in the worst case when PSS and TCSC is out of work, the damping torque becomes negative. The oscillation frequency of rotor with and without controllers for selected situation A, B and C is shown in Table 4. As shown in Table 4 when PSS and TCSC is out of work the oscillation frequency of rotor is positive and the system lose its stability following a severe disturbance. By increasing the gain of PSS and TCSC controllers the damping torque increases while the synchronizing torque decreases. So the designer should trade of between synchronizing and damping torques and select the appropriate values within limits so all objective functions are satisfied and overall stability is ensured.

Table 4. Oscillation frequency of rotor without and with controllers for selected situation A, B and C

without PSS and TCSC	with PSS and TCSC		
	A	B	C
$0.164 \pm j9.565$	$-0.77 \pm j9.48$	$-2.72 \pm j7.96$	$-3.5 \pm j5.12$

As shown in Table 4, the oscillation frequency of rotor with controllers in situation C has smaller real part rather than others, so in situation C the disturbance should be damped faster than A and B. The variation of rotor's speed and rotor's angle for a disturbance that occurred in the transmission line are shown in Fig.9 and Fig.10.

As shown in figure in situation C the disturbance is damped faster than A and B.

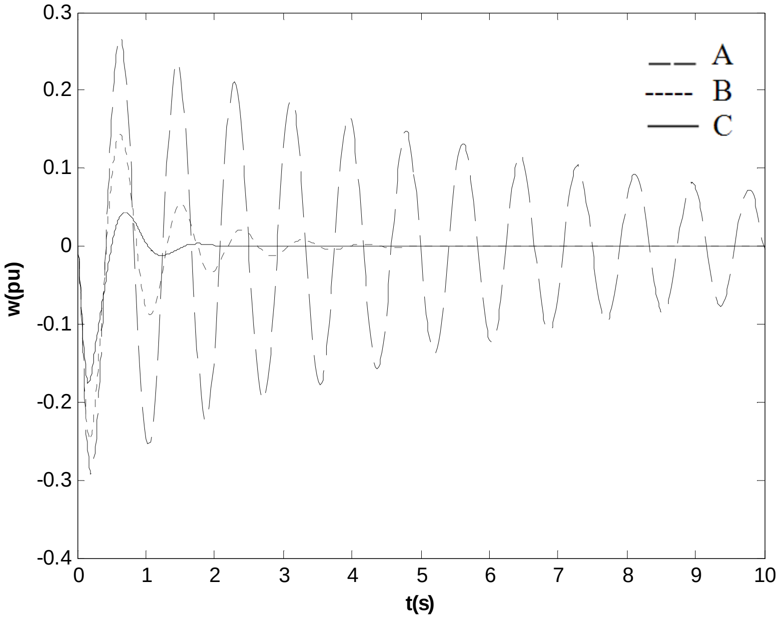

Fig. 9. The variation of rotor's speed after occurring a disturbance in transmission line

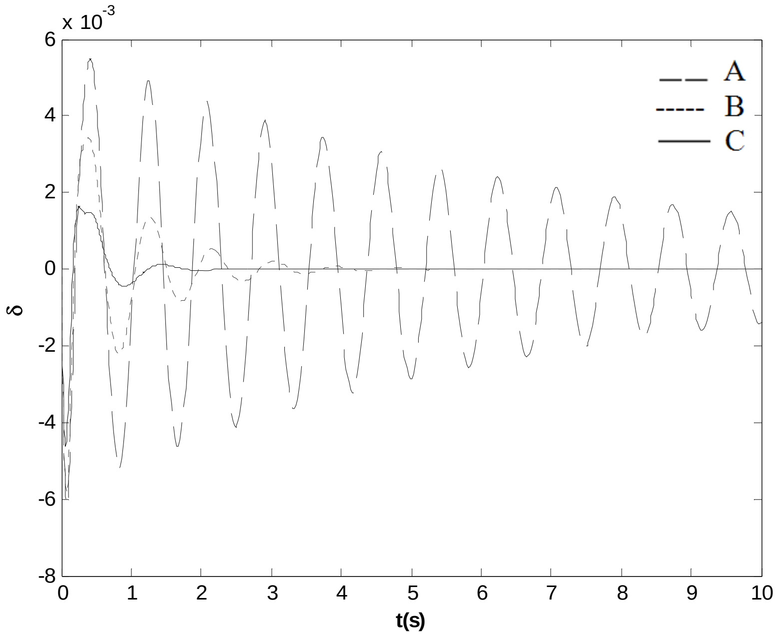

Fig. 10. The variation of rotor's angle after occurring a disturbance in transmission line

7. Conclusion

In this paper, in order to provide the dynamic stability of a SMIB system simultaneous coordination of PSS and TCSC controllers are presented. Although in dynamic stability enhancement the power system oscillation damping is intended but its stability to be retained following sever disturbances. Hence in this study the problem of simultaneous controllers design is considered as an optimization problem in which synchronizing and damping torques are the objective functions. Since these two objective functions are acted contradictory so multi objective genetic algorithm based Pareto front is considered to optimize these objective functions. By this approach we obtained a set of solutions that represent optimal coordination of PSS and TCSC in different conditions. The controllers are tested on weakly connected power system. The simulation results are presented and analyzed for different obtained solutions.

Appendix

The system test data are as follow (all data are in pu unless specified otherwise):
Generator: H=5s, D=0, r_a=0.003, X_d=0.9, X_q=0.55, X'_d=0.25, T'_{do}=5, $\delta_0 = 36^\circ$, P_e=0.93, Q_e=0.3, f=60.
IEEE Type-ST1A excitation system: K_A=200, T_A=0.05.
Transmission line and Transformer: X_L = 0.6, X_T = 0.1.
TCSC Controller: X_C=0.35, X_P=0.062, $\sigma_0 = 45^\circ$.

References

[1] F. P. Demello & C. Concordia, Concepts of synchronous machine stability as affected by excitation control, *IEEE Transactions on Power Apparatus and Systems*, *88*, 316-329, 1969.

[2] M. J. Gibbard, D. J. Vowles & P. Pourbeik, Interactions between, and effectiveness of, power system stabilizers and FACTS device stabilizers in multimachine systems, *IEEE Transactions on Power Systems*, *15*, 748-755, 2000.

[3] N. Mithulananthan, C. A. Canizares & J. Reeve, Tuning, performance and interactions of PSS and FACTS controllers, *IEEE Power Engineering Society Proceeding*, 981-987, 2002.

[4] P. Mattavelli, G. C. Verghese & A. M. Stankovitctt, Phasor dynamics of Thyristor-Controlled series capacitor systems, *IEEE Transaction on Power Systems*, *12*, 1259-1267, 1997.

[5] T. J. E Meiller, *Reactive Power Control in Electric System*, John Wiley and Son, 1982.

[6] Y. N. Yu, *Power System Dynamics*, Academic press, London, 1983.

[7] J. J. Sanchez-Gasca & J. H Chow, Power system reduction to simplify the design of damping controllers for inter-area oscillations, *IEEE Transactions on Power Systems*, *11*, 1342-1349, 1996.

[8] P. Pourbeik & M. J. Gibbard, Simultaneous coordination of power system stabilizers and FACTS device stabilizers in a multimachine power system for enhancing dynamic performance, *IEEE Transactions on Power Systems*, *13*, 473-479, 1998.

[9] Y. L. Abdel-Magid & M. A. Abido, Robust coordinated design of excitation and TCSC-based stabilizers using genetic algorithms, *International Journal of Electrical Power & Energy Systems*, *69*(2), 129-141, 2004.

[10] S. Panda & N. P. Padhy, Power System with PSS and FACTS Controller: Modeling, Simulation and Simultaneous Tuning Employing Genetic Algorithm, *International Journal of Electrical, Computer, and Systems Engineering*, *1*(1), 9-18, 2007.

[11] K. R. Padiyar, Power system dynamics: stability and contro”l. New York: John Wiley & Sons, 1996.

[12] R. M. Mathur & R. K. Varma, *Thyristor-based FACTS Controllers for Electrical Transmission Systems*, IEEE Press, Piscataway, 2002.

[13] P. Kundur, *Power System Stability and Control*, New York: McGraw-Hill, 1994.

[14] J. H. Holland, *Adaptation in nature and artificial system*, MIT Press, Cambridge, 1992.

[15] E. Goldberg, *Genetic Algorithms in Search, Optimization & Machine Learning*, Addison-Wesley: Reading, 1989.

[16] C. M. Fonseca & P. J. Fleming, Genetic Algorithms for Multi objective Optimization: Formulation, Discussion and Generalization, *Fifth International Conference on Genetic Algorithms,* 1993.